Proceedings of 2009 ASME Pressure Vessels and Piping Division Conference
PVP2009
July 26-30, 2009, Prague, Czech Republic

PVP2009-77734

GASEOUS DETONATION IN PIPING SYSTEMS PARTIALLY FILLED WITH LIQUID

Joseph E. Shepherd*and R. Akbar
Graduate Aeronautical Laboratories
California Institute of Technology
Pasadena, California, 91125

E. A. Rodriguez
Global Nuclear Network Analysis, LLC
Box 4850
Los Alamos, NM 87544

ABSTRACT

In this paper, we report the results of our investigation into the transmission of a detonation from a gas-filled section of pipe into a water-filled portion. Experimental studies were performed using a detonation in a H_2-N_2O mixture within a 2-inch, Schedule 40 pipe. The detonation wave impinges on a vertical column of water just downstream of a 90-degree bend. A shock wave is transmitted into the water-filled section and propagates slower than the sound speed in the water due to the coupling of flexural waves in the pipe with pressure waves in the liquid. Incident, transmitted, and reflected pressures in the gas are monitored, along with hoop and longitudinal strain throughout the pipe length. Results are presented for a both prompt initiation of an ideal (Chapman-Jouguet) detonation and deflagration-to-detonation transition (DDT) occurring just upstream of the gas-liquid interface. The results of the experiments are analyzed using computational modeling and simulation with an Eulerian hydrodynamic code as well as classical wave interaction methods. For a Chapman-Jouguet (CJ) detonation, the reflected and transmitted pressures agree with the classical one-dimensional theory of wave interaction. The values of the peak reflected pressure are close to those that would be obtained considering the water as a perfectly reflecting boundary. The transmitted wave propagates at a speed consistent with the Korteweg speed of classical water hammer theory and little to no attenuation in amplitude over $\sim$ 1.5 m of travel. In one DDT event, peak pressures up to 11 times the CJ pressure were observed at the end of the water-filled section.

INTRODUCTION

Gaseous detonations in piping systems are a potential and real hazard in both the petrochemical and nuclear industries. Notable examples of piping failures resulting from internal explosions were reported at Hamaoka-1 NPP [1, 2] and Brunsbuettel KBB [3], resulting from generation of a H_2-O_2 mixture by radiolysis, which further accumulated in stagnant pipe legs since these piping configurations lacked high-point vents or off-gas systems. In those cases, the piping failure was attributed to extreme pressures developed by deflagration-to-detonation transition occurring near an elbow close to the surface of the water-filled portion of the pipe. Factors contributed to the failures are believed to include pressurization during the flame propagation stage followed by detonation wave reflection from the water surface and bend.

Laboratory testing and analysis during the last decade, reviewed by Shepherd [4], has advanced our understanding of structural loading for relatively ideal situations of straight pipe runs filled with explosive gases. However, industrial power and processing plants contain many other features such as bends and liquid or slurry-filled pipe portions that may play a significant

*Address all correspondence to this author.

role in determining the structural loading. This study extends the previous work to examine these non-ideal features and is part of a larger effort to provide guidance for the design of piping systems with potential internal explosion hazards. Our goals in the part of the study presented in this paper are to characterize the detonation interaction at the gas-water interface and to determine the magnitude of the peak pressures in the gas and strains in the piping system. In the course of our work, we have examined the application of simple models for detonation reflection and shock wave propagation for the estimation of hoop and axial strains in the piping system. In addition, we have used a multi-material shock wave physics simulation tool to probe the details of the fluid-structure interaction.

EXPERIMENTAL APPARATUS AND TEST PROCEDURE

Our tests are carried out in an instrumented piping system partly filled with water. The piping system (Fig. 1) was fabricated from 304 stainless steel, schedule 40, 2-in ASTM 312 type commercial pipe and 300 lb class slip-on flanges, see Table 1. The flanges and one joint just upstream of the bend were joined by welding certified to ASME B31.3 standards. The pipe had a nominal outer diameter of 60.3 mm and a wall thickness of 3.81 mm.

Table 1. 2-in Schedule 40 Type 304 Stainless Steel pipe, nominal properties.

Outer diameter	60.3	mm
Inner diameter	52.5	mm
thickness h	3.912	mm
Mean radius R	28.2	mm
Young's modulus E	1.93×10^{11}	Pa
mass density ρ	8040	kg/m^3
Poisson ratio ν	0.305	
Specific heat capacity C_p	500	J/kg-K
Thermal expansion coefficient (linear) α	$16.9 \times 10{-}6$	K^{-1}
Thermal conductivity k	16.2	W/m-K
hoop frequency f_{hoop}	29.0	kHz

The piping system was made up of two segments butt welded just upstream of a 90-degree bend as shown in Fig. 1. The horizontal run is approximately 3.5 m, followed by the bend and a vertical section of approximately 1.5 m. The bend was made using a hydraulic bending machine and a mandrel to create a 19.3 cm radius (centerline of pipe) bend connecting the vertical and horizontal segments. The pipe was instrumented with bonded strain gages at selected locations and oriented as shown in Fig. 1. Piezo-electric pressure transducers were flush-mounted along the side and at the end of the pipe. The strain gages were operated in quarter-bridge mode using a Vishay 2310B signal conditioner operated in the wide-band (140 kHz, -3 dB point) mode. The pressure gages are fast-response (rise times on the order of 1 μs) units (PCB 113A type) designed for shock wave measurements. Pressure and strain signals were recorded with a 14-bit transient digitizer at a sample interval of 1 μs per point.

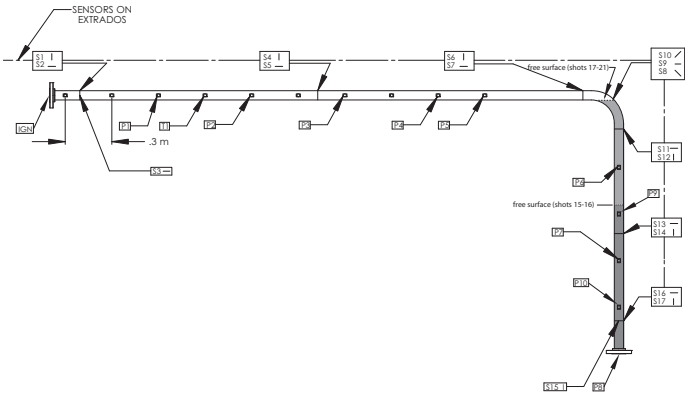

Figure 1. Experimental test fixture showing pipe and sensor locations.

The procedure was to first evacuate the piping system to less than 40 mTorr), fill the pipe with the test mixture (H_2 and N_2O) using the method of partial pressures, and mix the gas by circulating it through the pipe using a bellows pump connecting the two ends. The total pressure of the gas at the end of the filling process was set to a value less than atmospheric so that after the water was added, the pressure within the pipe would be 1 atm. After mixing the gas, the pipe was closed off at each end with ball valves and a secondary valve used to introduce water at the lowest point of the vertical leg of the piping system. The water was supplied by a carboy mounted next to the pipe system with sufficient head to insure that we could reach the desired level of the free surface within the pipe.

Two sets of water levels were used in a series of tests that examined the effect of water level, gas composition, and ignition method. The combustion event was started with an ordinary spark plug. In order to investigate ideal detonations, a short (305 mm) insert of coiled spring or Shchelkin spiral was used to accelerate the flame quickly to a detonation for a 30% H_2 and 70% N_2O mixture (see Table 4 for detonation parameters). The spiral was removed in order to test deflagration-to-detonation transition (DDT) events with lower concentrations of H_2.

Results

We carried out a set of 7 tests with water in the vertical leg. Four of the tests (15-18) were with the Shchelkin spiral to promptly create CJ detonations and three tests (19-21) used spark ignition without the spiral to examine DDT events. Two water levels were used as shown in Fig. 1 and the specific test conditions are described in Table 2. In addition to these tests, a number (a total of 36) of other tests were carried out to obtain data on pipes without water in order validate models of forces induced by the detonation propagation around the bend and reflection from the pipe end. Test 3 provides reference data for comparison of strains and pressures without water in the vertical leg.

Table 2. Test conditions. For all tests, the initial pressure P_o = 101.3 kPa and temperature T_o = 27 °C.

test	H_2	N_2O	U_{CJ} (m/s)	P_{CJ} (MPa)	Spiral	Water (cc)
3	0.30	0.70	2087.5	2.62	Y	0
15	0.30	0.70	2087.5	2.62	Y	2250
16	0.30	0.70	2087.5	2.62	Y	2250
17	0.30	0.70	2087.5	2.62	Y	3750
18	0.30	0.70	2087.5	2.62	Y	3750
19	0.17	0.83	1917.5	2.57	N	3750
20	0.15	0.85	1891.9	2.56	N	3750
21	0.17	0.83	1917.5	2.57	N	3750

CJ Detonation

No water Test 3 was carried out with only gas within the pipe and gives base line data that we can compare to the cases with water in the vertical leg. Referring to Figs. 2 - 4, we observe that the detonation was initiated at the left side of the pipe system and propagates with a constant velocity (within 1% of the CJ velocity given in Table 4) and is nearly unaffected by the bend. We estimate the detonation cell width is about 3 mm in this mixture [6], sufficiently small that the detonation will behave in a relatively ideal fashion. At the lower right-hand side of the pipe system, the detonation reflects from the closed end of the pipe and a shock wave proceeds back toward the ignition end. The peak strains in the pipe are in the hoop direction and about 200-300 μstrain in magnitude, which corresponds to a dynamic load factor of 2 to 2.5 applied to the CJ pressure and modeling the hoop response as a single degree of freedom harmonic oscillator.

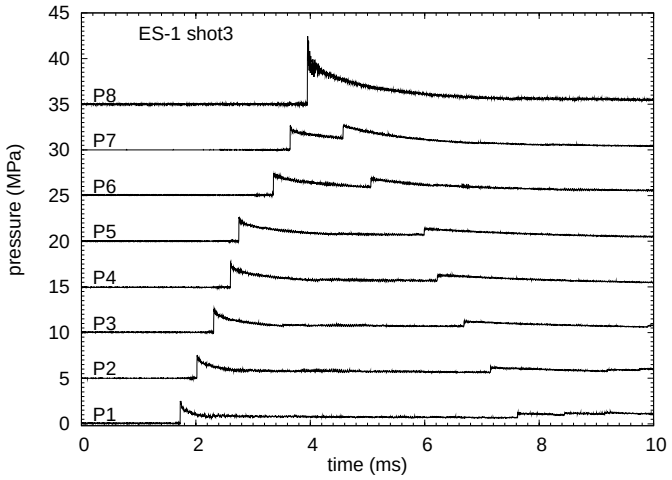

Figure 2. Test 3 pressure measurements.

2250 cc water We filled the the lower portion of the vertical leg of the pipe system with about 2250 cc of water in tests 15 and 16, reaching the lower level shown in Fig. 1. The total pressure before adding the water was about 617 Torr and after filling, 760 Torr. The nominal water level was just above pressure gage P9 and the total length of the water column was about 0.97 m as measured from the gage P8 at the bottom of the vertical section. Pressure and strain data are shown for test 15 in Figs. 5–7 for the same sensor locations as in test 3.

The pressure data (Fig. 5) show a transmitted shock wave

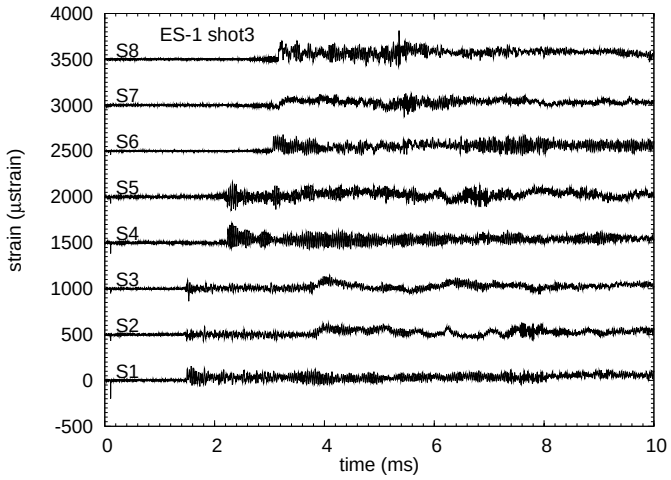

Figure 3. Test 3 strain gage set 1 measurements.

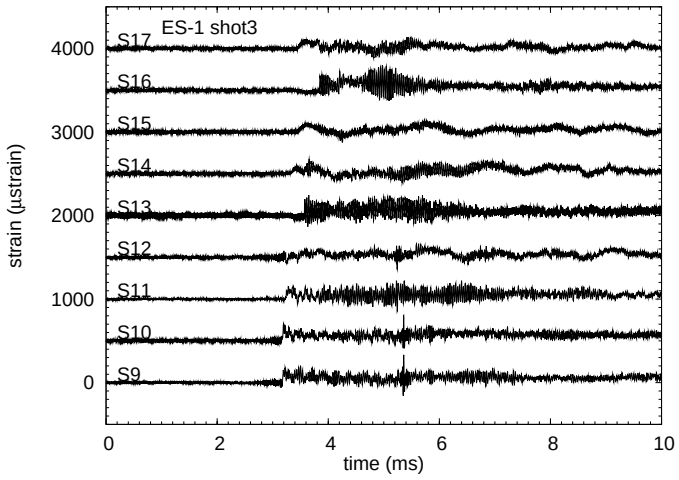

Figure 4. Test 3 strain gage set 2 measurements.

in the water and a reflected shock wave in the gas. The peak pressures of the incident waves in the gas (2.7 MPa vs. a CJ pressure of 2.5) and water (6 MPa) are consistent with standard detonation wave-free surface interaction analysis using pressure-velocity diagrams, described in [7]. The analysis (Fig. 8) predicts a peak pressure in the water (6.35 MPa) that is almost identical to the peak pressure (6.4 MPa) obtained in reflecting the detonation from a hard surface. The propagation speed of the detonation is within 0.5% of the CJ velocity (see the x-t diagrams in Fig. 9) and the propagation of the lead shock wave in the water is about 1310 m/s, substantially slower than the shock speed in water alone[1] due to the coupling of the pressure wave in the water with the stress waves in the pipe, see [8] and discussion of the numerical results below. The peak strains (Fig. 7) in the water-filled segment are similar to those observed at the same location in the gas-filled test (Fig. 4). Although the pressures are higher, the wave speeds in the water-filled case are lower than for the gas-filled case. The lower wave speeds and the effect of fluid-structure coupling results in lower strains in water-filled section than would be expected on the basis of peak pressure alone.

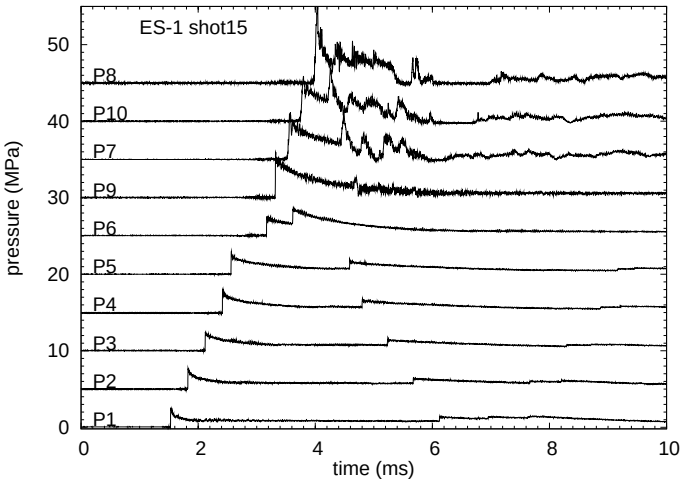

Figure 5. Test 15 pressure measurements.

The amplitude of the shock wave in the water does not appreciably attenuate in the $\sim$1 m of travel between the free surface and the bottom of the pipe (Fig. 5) although there is an expansion wave following the shock. The shock wave in the water reflects from the bottom and the peak amplitude (10.7 MPa) is slightly lower than double the incident wave (see signal P8 of Fig. 5). This is consistent with transmission of a wave into the steel supporting structure at the bottom of the pipe. Although this structure is very stiff, it is not completely rigid and in addition to the standard wave interaction processes at the water-steel interface, there will be some flexing of the support structure. The reflected

[1]The shock speed obtained in a ideal one-dimensional test will be only slightly (10-40 m/s) higher than the sound speed of 1480 m/s for the pressure amplitudes encountered in the present cases.

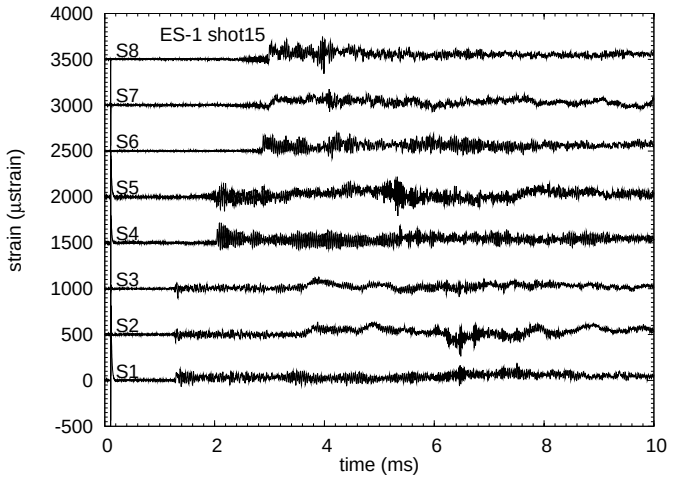

Figure 6. Test 15 strain gage set 1 measurements.

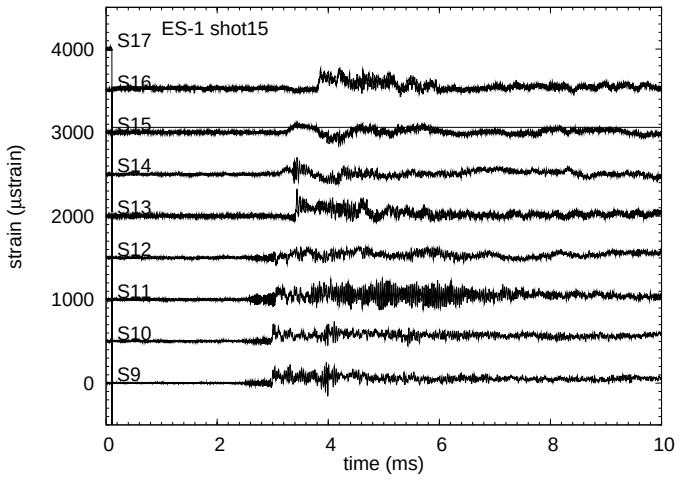

Figure 7. Test 15 strain gage set 2 measurements.

wave rapidly attenuates as it moves through the pressure drop in the expansion wave.

After the reflected shock reaches the free surface of the water, it reflects with a change in sign and creates a tension wave that propagates back to the bottom on the pipe. The amplitude of the tension wave increases on reflection from the bottom and causes cavitation of the water. The presence of cavitation is signaled by the portions of the pressure signal that are flat and close to or below zero in gages P8, P10, and P7 between 5.8 and 7 ms in Fig. 5. Since the pressure measured by the gages is relative to the initial pressure in the pipe (101 kPa), a level less than -0.1 MPa corresponds to tension in the water. The greatest tension was observed on gage 10 of Fig. 5, for which the average gage pressure between 6.2 and 6.6 ms is approximately -0.23 MPa for an absolute tension of -120 kPa. The lowest pressures observed on the other gages ranged from +20 to + 70 kPa. By comparison, the vapor pressure of water is 3 kPa at 297°C.

The location of the free surface of the water was not directly measured but we can use an x-t diagram (Fig. 9) to extrapolate the wave trajectories to estimate the location of the free surface from the intersection of the trajectories. The trajectories were estimated using a linear least squares fit of the arrival time-distance data. As shown in the enlarged x-t diagram in Fig. 9, the free surface was approximately 30 mm above gage P9. There is some uncertainty in this value but from the appearance of the pressure signals, it is clear that gage P9 was submerged in the water.

The strain gage records (S13-S16) in the water-filled section (Fig. 7) are similar in overall appearance to the corresponding gages in the gas-only test (Fig. 4). The strains are slightly lower in peak amplitude and the high frequency oscillations are significantly damped in comparison to the tests without water. The longitudinal strain wave precursor on S15 and S14 (gage S17 failed on test 15) is almost identical to the precursor in the gas only tests, confirming that this signal is associated with the detonation wave propagating through the elbow. The strain signals in the water-filled section are consistent with those observed in separate tests carried out at Caltech using impact to generate stress waves in water-filled tubes [8].

3750 cc water In tests 17-21, more water was added than in 15-16 so that the nominal water level was just below the bottom of the horizontal piping segment and within the bend itself as shown in Fig. 1. The total length of the water column was about 1.77 m as determined by the interpolating time of arrival data on an *x-t* diagram. In tests 17 and 18, the detonation was initiated using the Shchelkin spiral so that a detonation rapidly formed in the horizontal segment and reflected from the water surface in a fashion that was similar to tests 15-16. The test data shown in Fig. 10 is qualitatively very similar to that shown in Fig. 5 with expected difference in arrival time due to the length of the water column. Test 18 was a replica of test 17 that demonstrated the reproducibility of the data. A better estimate of the water shock wave speed can be obtained in these tests due to the larger number of transducers in the water. A water shock wave speed of 1370 m/s, close to the predicted Korteweg speed is observed in

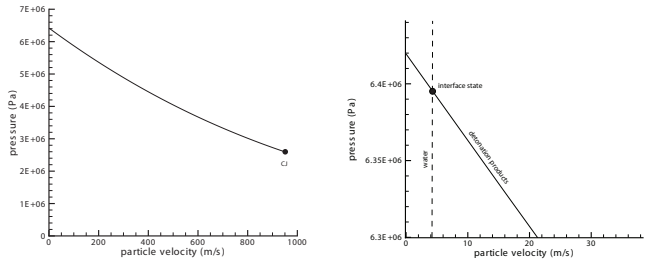

Figure 8. Pressure-velocity diagrams for shock wave propagation in detonation products behind a detonation in H_2/N_2O (30/70 mixture at 1 atm initial pressure, 295 K). a) Complete range of flow speed behind the detonation. b) Enlarged view of region near axis with water shock adiabatic (nearly vertical dashed line) showing solution for detonation reflection on water free surface. See Browne et al. [5] for details.

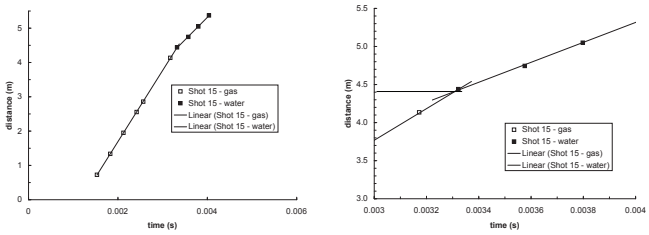

Figure 9. Distance-arrival time (x-t) plots for test 15 showing detonation wave in gas (2075 m/s) and shock wave in water (1310 m/s). Right hand figure is an enlargement showing extrapolated location of free surface of water.

tests 17 and 18. The peak strains (not shown) are very similar for all gages except 8, 9, and 10 which are located on the extrados of the bend half-way between the vertical and horizontal piping segments. The higher strains in tests 17 and 18 occur at this location since the reflected wave is strongest just above the location of the water free surface.

Deflagration and DDT

Tests 19, 20, and 21 were carried out without the Shchelkin spiral and with lower concentrations of H_2 in order to create conditions for deflagration-to-detonation transition near the water surface. In test 19, see Figs. 11–13, a very clear DDT event is observed, with peak pressures (Fig. 16) of 14 MPa in the transmitted shock in the water and up to 30 MPa upon reflection from the end of the vertical section. Peak strains (Fig. 17) of up to

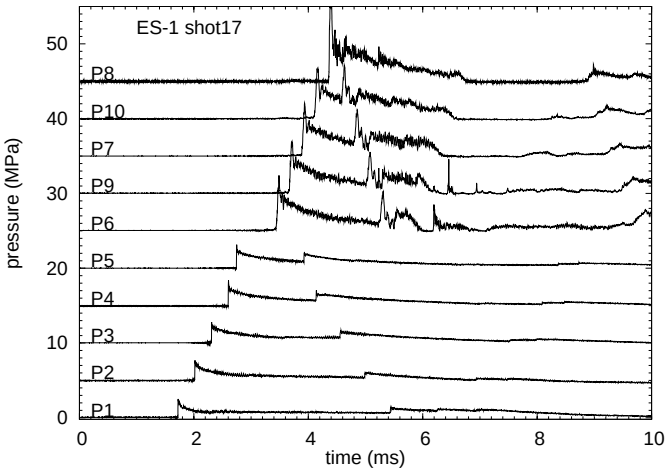

Figure 10. Test 17 pressure measurements.

1000 μstrain are observed in both gas-filled section and up to 700 μstrain in the liquid-filled section. Only a deflagration occurred in test 20 (Fig. 14) and resulting peak pressures (Fig. 16) are only about 1/2 the CJ value and the peak strains are between 50-100 μstrain. Test 21 was intended to be a replica of test 19 but due to the variability of the DDT process, the event in test 21 was much weaker and the resulting pressures (Fig. 15) and strains are more similar to CJ values than the extremes observed in test 19. The strains and peak pressures observed in test 19 are similar to those in test 9 (not shown) which was carried out without water and at a concentration of 15% H_2. The event in test 19 is of the type that has been proposed as occurring in the Hamaoka NPP and led to the catastrophic failure of the NPP piping near a bend.

Numerical Simulation

A numerical simulation of a H_2-N_2O detonation wave impacting a liquid surface was developed with the aid of shock-wave propagation code, CTH. CTH is a multi-material, large deformation, strong shock-wave, solid mechanics code developed at Sandia National Laboratories [9, 10]. CTH has models for multiphase, elastic-viscoplastic, porous, and explosive materials. Three-dimensional rectangular meshes, two-dimensional rectangular and cylindrical meshes, and one-dimensional rectilinear, cylindrical, and spherical meshes are available. It uses second-order accurate numerical methods to reduce dispersion and dissipation and to produce accurate, efficient results. Hydrodynamic codes, as the name implies, are based on the funda-

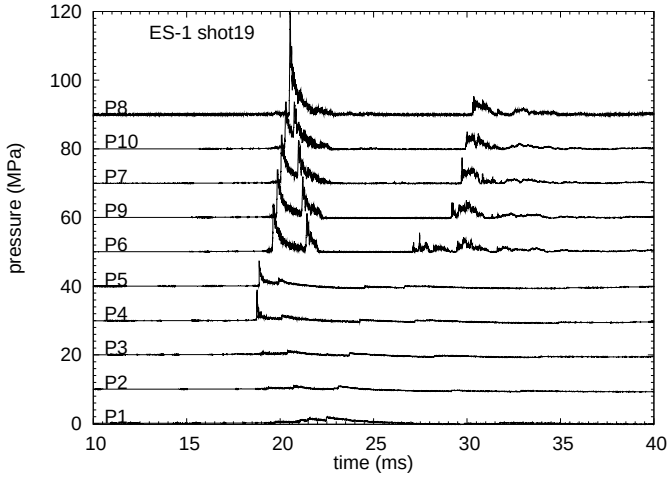

Figure 11. Test 19 pressure measurements.

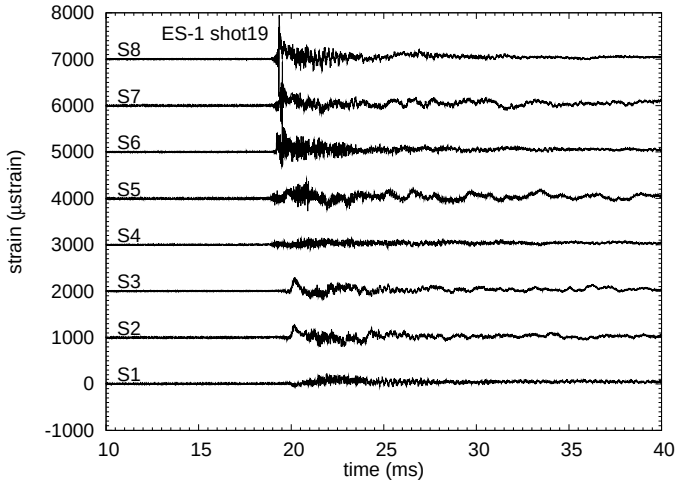

Figure 12. Test 19 strain gage set 1 measurements.

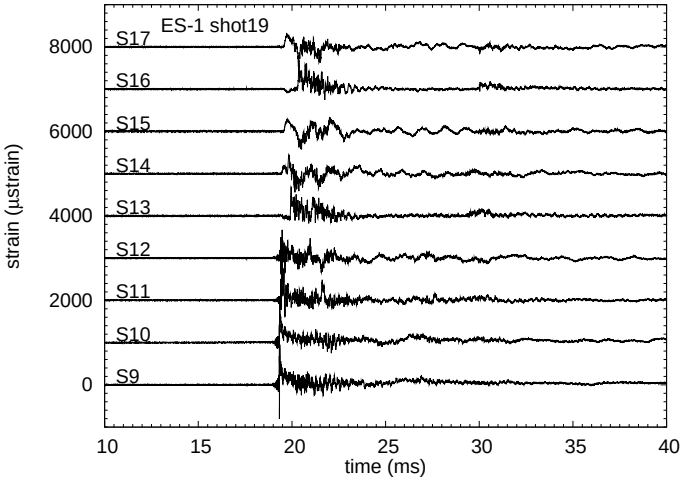

Figure 13. Test 19 strain gage set 2 measurements.

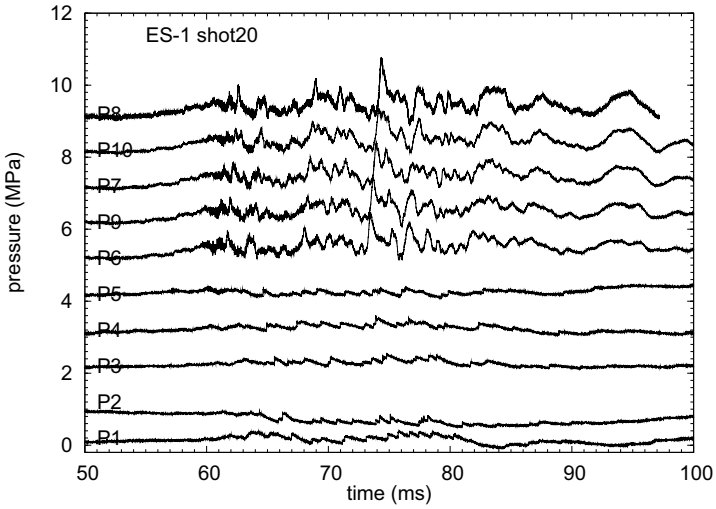

Figure 14. Test 20 pressure measurements.

mental equations of fluid dynamics; conservation of mass, momentum, and energy. The goal is to determine certain features associated with the detonation wave, specifically the incident, reflected, and transmitted pressures from the liquid surface, and the incident and reflected pressures at the closed-end of the piping run. Further, we endeavor to gain additional insight relative to precursor stresses developed in the pipe wall, which are generated from a traveling detonation front.

Materials and Equations-of-State

The properties listed in Table 3 are utilized in the hydrocode model for the separate materials and detonation condition. It should be emphasized that the 304L stainless steel pipe encompasses both the hydrostatic and deviatoric response. The hydrostatic (or spherical) portion is defined by the equation-of-state (EOS) for steel, and the deviatoric portion is defined by the constitutive behavior, i.e., stress-strain representation. The Steinberg-Guinan constitutive model was utilized due to its ro-

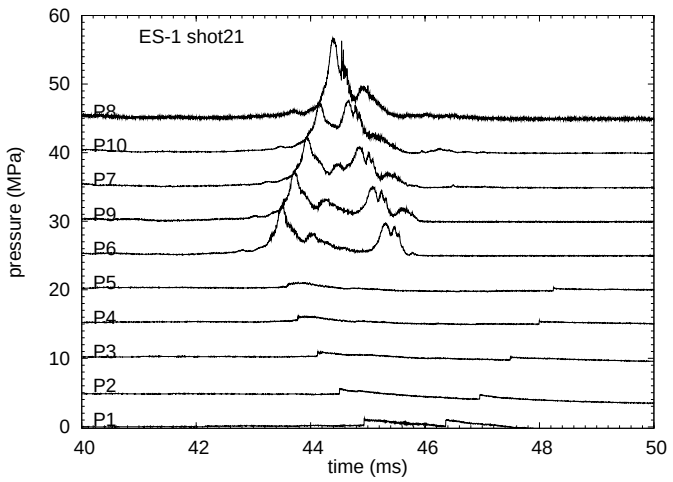

Figure 15. Test 21 pressure measurements.

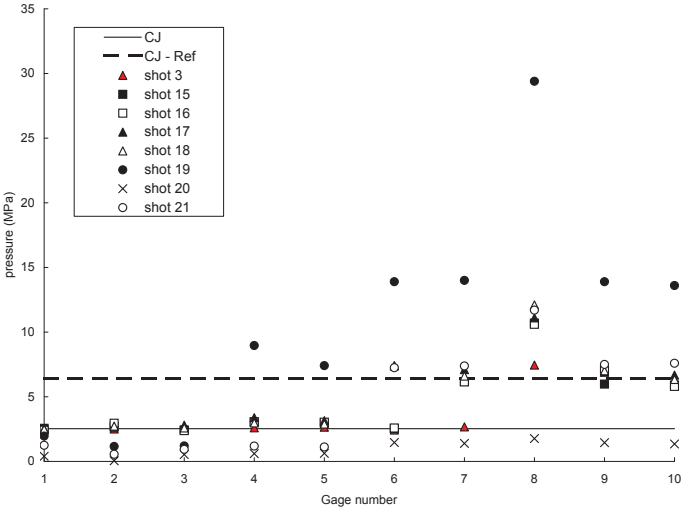

Figure 16. Peak pressures on all gages. CJ - computed ideal CJ detonation pressure, CJ - Ref - computed ideal reflected CJ detonation pressure.

bust capability in the viscoplastic region. Although the model is robust and quite accurate for 304L stainless steel, the penalty associated with such a model is the longer run-times. The detonation products are modeled with the JWL EOS, which at the pressures of interest is simplified to be just the ideal gas model. The SESAME EOS for water was used with a cavitation threshold of -2 MPa, substantially lower that what was observed in

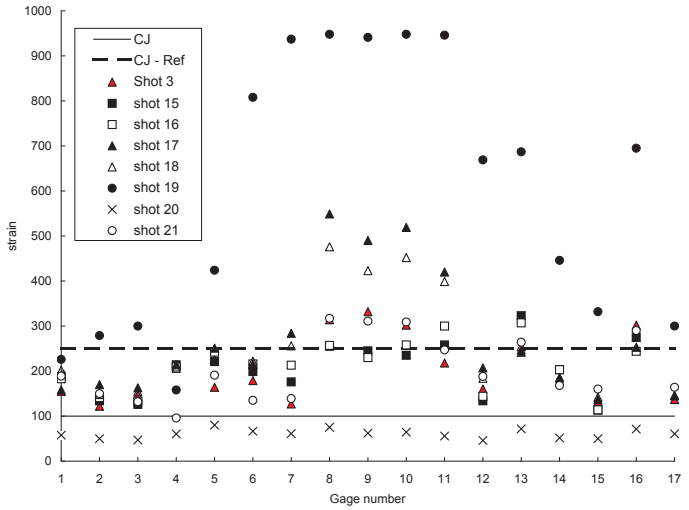

Figure 17. Peak strains on all gages; reference strains are computed using membrane stress and a dynamic load factor of 1.

the experiment. Cavitation phenomena will therefore not be correctly reproduced but this is not the focus of the present study.

Geometric Configuration

Figure 18 shows a representation of the piping system utilized in the numerical model. The simulation geometry did not include the bend shown in Fig. 1 but did model the entire length of piping equivalent to the experimental apparatus. That is, the total volume of fuel and oxidizer in the experimental apparatus was duplicated in the numerical model, including the point of ignition. This treatment was adopted to maintain a 2D approximation and thus ensure a tractable solution. The vertical segment of piping up to approximately 127 cm, contained a column of water. The Eulerian mesh is subdivided into 0.5-mm cell sizes from the closed-end (Datum) to 160-cm height of piping. This approach was taken to obtain a high-fidelity resolution of pressures and densities within the gas region, detonation front at gas-liquid interface, water column, and pipe wall. The remainder of the pipe length from 160-cm to the ignition end at 542-cm, received slightly coarser mesh sizing of 2.5-mm cells to alleviate excessive run-times.

Tracer particles are located within the Eulerian mesh to access state variables during the transient event. Tracer particles within the gas or liquid are offset from a symmetry or structural boundary to minimize the cell-averaging. For example, a boundary may have both liquid cells and steel structure; however, it

Table 3. Equation of state and constitutive model parameters used in CTH simulations.

Equation of State Parameters			
Material	Density	Sound Speed	EOS model
	(kg/(m^3)	(m/s)	
304L Steel	7.896×10^3	4569	Mie Gruneisen
Water	1.000×10^3	1480	Sesame
H_2-N_2O	1.2754	-	JWL
Steinberg-Guinan Strength Model			
Material	Modulus	Shear Modulus	Yield
	(GPa)	(GPa)	(MPa)
304L Steel	200.	77.0	340
JWL detonation Parameters for $0.3H_2$-$0.7N_2O$			
γ	P_{CJ}	D_{CJ}	T_{CJ}
	(MPa)	(m/s)	(K)
1.1566	2.7	2088	3385

would be erroneous to average the "pressure" or "density" from adjacent cells because these are different materials and different equations-of-state. As such, when determining actual pressure, velocity, and density, in either the gas or liquid, tracer particles are placed at 1.5 cell-widths from the boundary.

CTH Results

Comparing Figs. 19 and 5, we observe that the simulation results reproduce qualitatively and quantitatively the general features observed in the experiment. The incident detonation, reflected pressure wave in the gas as well as the transmitted and reflected shock waves in the water are clearly shown. The wave speeds and amplitudes are consistent with those observed in the experiment and the theoretical analysis of wave interactions with the water-gas interface. In particular, by tracking the peak pressure of the reflected shock wave in the gas, we can extrapolate to determine that the peak pressure created by detonation reflection at the water surface is 6.4 MPa essentially identical to the value given by the analysis leading to Fig. 8. The pressure signals in the water-filled section show very substantial fluctuations and there are pressure spikes near the gas-water interface that

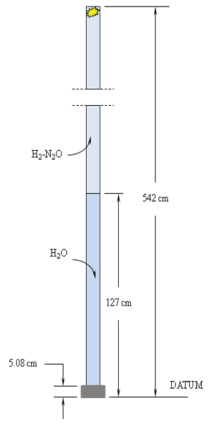

Figure 18. Geometry for numerical simulations.

appear to be artifacts that are much larger in magnitude than any fluctuations that are observed in the experimental data.

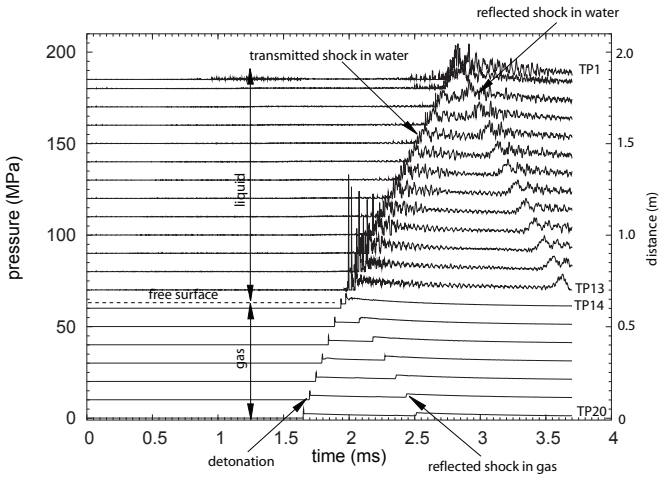

Figure 19. Pressure histories for 20 locations - numerical simulations.

The details of the interaction of the detonation wave with the pipe wall are shown in Fig. 20. The pressure of the detonation wave in the gas creates radial and longitudinal stress waves in the pipe wall. The main stress in the pipe is due to radial deflection and the hoop strain front propagates with the detonation speed in gas-filled pipes as discussed by Beltmann and Shepherd [11]. In addition, a series of oscillatory precursor waves can be observed

ahead of the main disturbance. The theoretical origin of the precursor waves is due to the propagation of longitudinal waves at the bar speed of about 5000 m/s, approximately 2.5 times faster than the detonation wave. The stresses predicted in the numerical simulations are consistent with the strains observed in the experiment, as shown in Fig. 3-4 and Figs. 6-7.

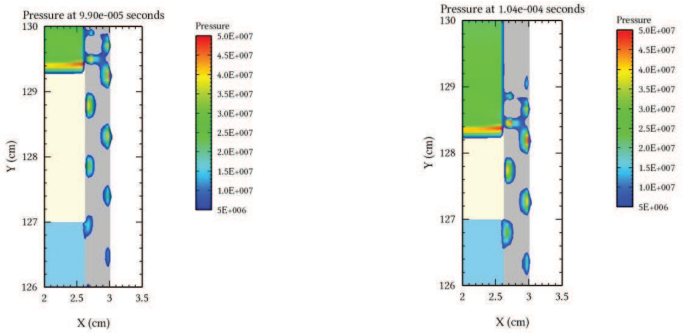

Figure 20. Interaction of detonation pipe wall to create stress precursor waves - numerical simulations.

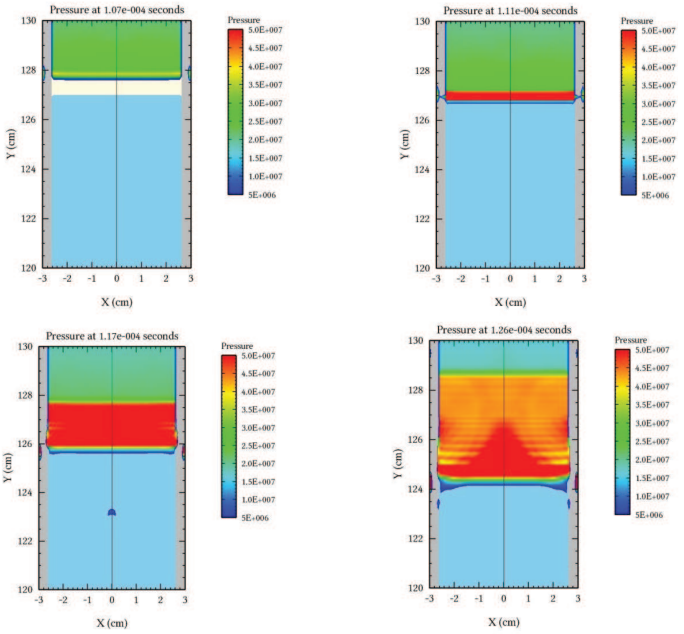

Figure 21. Interaction of detonation with water free surface - numerical simulations.

Snapshots of the interaction of the detonation wave with the water-gas interface are shown in Fig. 21. The interface remains nearly planar as do the initial transmitted and reflected shock waves. An oscillatory structure can be observed close to the interface which subsequently develops into an extended oscillatory precursor wave that is shown in Fig. 22.

The theory of wave propagation in water-filled pipes has been developed in the context of water hammer by Skalak [12]. The shock wave propagating in the water is coupled with the radial deformation wave in the pipe wall to an extent that depend of the effective stiffness in the pipe as compared to the compressibility of the water [8]. As a consequence, the coupled wave system propagates with the Korteweg speed, 1370 m/s in the present case, which is slower than either the sound speed in the water or the bar speed in the pipe. Skalak's theory also predicts a precursor wave propagating at close the bar speed and consisting of primarily longitudinal strain. The results shown in Fig. 22 reveal that the precursor wave is actually a complex structure with radial and longitudinal spatial oscillations extending a substantial distance ahead of the main disturbance. These oscillations are induced in the water by the oscillation of the pipe wall associated with the precursor waves shown in Fig. 18. However, the magnitude is quite small and only a small amplitude oscillation can be observed ahead of the main pressure jump on gages P9, P10, and P8 in Figs. 5 and 10. The oscillations are stronger behind the main pressure front and this gives rise to the noisy appearance of the signals on pressure gages in the water-filled section as compared to the pressure gages in the gas-filled section.

Conclusion

Detonations reflecting from the free surface of a water-filled section produce peak reflected shock pressures (Fig. 16) that are comparable to reflection from a rigid surface. The transmitted shock waves in the water maintain their shape and peak amplitude with minimal attenuation a substantial distance from the water surface. The transmitted shock in the water propagates close to the Korteweg speed predicted by the theory of water hammer. The peak strains (Fig. 17) are comparable for the gas and water-filled cases. Peak strains and pressures observed in a DDT event are comparable in piping with and without water-filled segments, with peak pressures up to 30 MPa and peak strains up to 1000 μstrain. The force on the pipe due to the detonation propagation around the bend is manifested as an axial strain wave propagating away from the bend at approximately the bar speed. On the downstream side of the bend, the axial strain wave can be

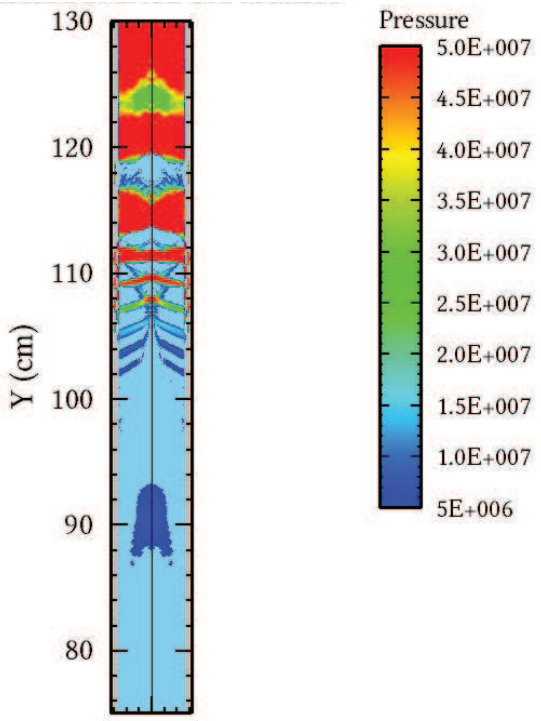

Figure 22. Pressure contours in water at 2.05 ms - numerical simulations.

observed propagating ahead of the detonation wave.

ACKNOWLEDGMENT

This research was sponsored by the US Department of Energy, Office of River Protection, Richland, WA.

REFERENCES

[1] Naitoh, M., Kasahara, F., Kubota, R., and Ohshima, I., 2003. "Analysis of pipe rupture of steam condensation line at Hamoaka-1, (I) Accumulation of noncondensable gas in a pipe". *Journal of Nuclear Science and Technology,* **40**(12), p. 1032.

[2] Naitoh, M., Kasahara, F., Kubota, R., and Ohshima, I., 2003. "Analysis of pipe rupture of steam condensation line at Hamoaka-1, (II) Hydrogen combustion and generation". *Journal of Nuclear Science and Technology,* **40**(12), pp. 1041–1051.

[3] Kuznetsov, M., Breitung, W., Grüne, J., and Singh, R. K., 2005. "Structural response of DN15-tubes under radiolysis gas detonation loads for BWR safety applications". In 18th International Conference on Structural Mechanics in Reactor Technology, no. SMiRT 18-J09-1.

[4] Shepherd, J. E., 2006. "Structural response of piping to internal gas detonation". In ASME Pressure Vessels and Piping Conference., ASME. PVP2006-ICPVT11-93670, presented July 23-27 2006, Vancouver BC Canada.

[5] Browne, S., Ziegler, J., and Shepherd, J. E., 2004. Numerical solution methods for shock and detonation jump conditions. Tech. Rep. FM2006.006, GALCIT.

[6] Pfahl, U., Schultz, E., and Shepherd, J., 1998. Detonation cell width measurements for H_2-N_2O-O_2-CH_4-NH_3 mixtures. Tech. Rep. FM98-5, GALCIT, April.

[7] Meyers, M. A., 1994. *Dynamic behavior of materials*. John Wiley & Sons.

[8] Inaba, K., and Shepherd, J. E., 2008. "Flexural waves in fluid-filled tubes subject to axial impact". In Proceedings of the ASME Pressure Vessels and Piping Conference. July 27-31, Chicago, IL USA. PVP2008-61672.

[9] McGlaun, J., Thompson, S., Kmetyk, L., and Elrick, M., 1989. A brief description of the three-dimensional shock wave physics code CTH. Tech. Rep. SAND89-0607, Sandia National Laboratory.

[10] McGlaun, J., Thompson, S., and Elrick, M., 1990. "CTH: A three-dimensional shock physics code". *International Journal of Impact Engineering,* **10**, pp. 351–360.

[11] Beltman, W., and Shepherd, J., 2002. "Linear elastic response of tubes to internal detonation loading". *Journal of Sound and Vibration,* **252**(4).

[12] Skalak, R., 1956. "An extension of the theory of water hammer". *Trans ASME,* **78**, pp. 105–116.

Table 4. Properties of CJ detonation in standard (0.3/0.7) H_2-N_2O mixture as computed with the Shock and Detonation Toolbox [5].

Initial conditions		
Pressure	100	(kPa)
Temperature	295	(K)
Density	1.2807	(kg/m^3)
sound speed a_1 (frozen)	319.2198	(m/s)
γ_1 (frozen)	1.3051	(m/s)
CJ state		
Wave speed	2088.0993	(m/s)
Pressure	2.63	(MPa)
Temperature	3383.	(K)
Density	2.343	(kg/m^3)
w_2 (wave frame)	1142.	(m/s)
u_2 (lab frame)	946.5	(m/s)
a_2 (frozen)	1187.0	(m/s)
a_2 (equilibrium)	1140.	(m/s)
γ_2 (frozen)	1.2542	(m/s)
γ_2 (equilibrium)	1.1566	(m/s)
Isentropic expansion to end of Taylor wave		
Pressure	0.958	(MPa)
Temperature	3005.	(K)
Volume	1.0218	(m3/kg)
Sound speed (frozen)	1107.2	(m/s)
Sound speed (equilibrium)	1065.4	(m/s)
γ (frozen)	1.2519	(m/s)
γ (equilibrium)	1.1593	(m/s)
Reflected Shock		
Speed	811.4	(m/s)
Pressure	6.529	(MPa)
Temperature	3784.	(K)